GEOPHYSICS, VOL. 64, NO. 3 (MAY-JUNE 1999); P. 800–808, 7 FIGS.

Multichannel analysis of surface waves

Choon B. Park*, Richard D. Miller*, and Jianghai Xia*

ABSTRACT

The frequency-dependent properties of Rayleigh-type surface waves can be utilized for imaging and characterizing the shallow subsurface. Most surface-wave analysis relies on the accurate calculation of phase velocities for the horizontally traveling fundamental-mode Rayleigh wave acquired by stepping out a pair of receivers at intervals based on calculated ground roll wavelengths. Interference by coherent source-generated noise inhibits the reliability of shear-wave velocities determined through inversion of the whole wave field. Among these nonplanar, nonfundamental-mode Rayleigh waves (noise) are body waves, scattered and nonsource-generated surface waves, and higher-mode surface waves. The degree to which each of these types of noise contaminates the dispersion curve and, ultimately, the inverted shear-wave velocity profile is dependent on frequency as well as distance from the source.

Multichannel recording permits effective identification and isolation of noise according to distinctive trace-to-trace coherency in arrival time and amplitude. An added advantage is the speed and redundancy of the measurement process. Decomposition of a multichannel record into a time variable-frequency format, similar to an uncorrelated Vibroseis record, permits analysis and display of each frequency component in a unique and continuous format. Coherent noise contamination can then be examined and its effects appraised in both frequency and offset space. Separation of frequency components permits real-time maximization of the S/N ratio during acquisition and subsequent processing steps.

Linear separation of each ground roll frequency component allows calculation of phase velocities by simply measuring the linear slope of each frequency component. Breaks in coherent surface-wave arrivals, observable on the decomposed record, can be compensated for during acquisition and processing. Multichannel recording permits single-measurement surveying of a broad depth range, high levels of redundancy with a single field configuration, and the ability to adjust the offset, effectively reducing random or nonlinear noise introduced during recording.

A multichannel shot gather decomposed into a swept-frequency record allows the fast generation of an accurate dispersion curve. The accuracy of dispersion curves determined using this method is proven through field comparisons of the inverted shear-wave velocity (v_s) profile with a downhole v_s profile.

INTRODUCTION

In most surface seismic surveys when a compressional wave source is used, more than two-thirds of total seismic energy generated is imparted into Rayleigh waves (Richart et al., 1970), the principal component of ground roll. Assuming vertical velocity variation, each frequency component of a surface wave has a different propagation velocity (called phase velocity, C_f) at each unique frequency (f) component. This unique characteristic results in a different wavelength (λ_f) for each frequency propagated. This property is called dispersion. Although ground roll is considered noise on body-wave surveys (i.e., reflection or refraction profiling), its dispersive properties can be utilized to infer near-surface elastic properties (Nazarian et al., 1983; Stokoe et al., 1994; Park et al., 1998a). Construction of a shear (S)-wave velocity (v_s) profile through the analysis of plane-wave, fundamental-mode Rayleigh waves is one of the most common ways to use the dispersive properties of surface waves (Bullen, 1963). This type of analysis provides key parameters commonly used to evaluate near-surface stiffness—a critical property for many geotechnical studies (Stokoe et al., 1994). As well, the near-surface v_s field can provide useful information about statics during body-wave data processing (Mari, 1984).

Presented at the 66th Annual Meeting, Society of Exploration Geophysicists. Manuscript received by the Editor August 15, 1997; revised manuscript received November 23, 1998.
*Kansas Geological Survey, University of Kansas, 1930 Constant Avenue, Campus West, Lawrence, Kansas 66047-3726. E-mail: park@kgs.ukans.edu; rmiller@kgs.ukans.edu; jxia@kgs.ukans.edu.

In the early 1980s, a wave-propagation method to generate the near-surface v_s profile, called spectral analysis of surface waves (SASW), was introduced (Nazarian et al., 1983). SASW uses the spectral analysis of ground roll generated by an impulsive source and recorded by a pair of receivers. This method has been widely and effectively used in many geotechnical engineering projects (Stokoe et al., 1994). The single pair of receivers is configured and reconfigured (based on wavelength calculations made during acquisition) as many times as necessary to sample the desired frequency range. Data are analyzed in the frequency domain to produce a dispersion curve by calculating the phase difference between each deployment of receiver pairs. The inclusion of noise during SASW measurements occasionally can be controlled using a set of empirical criteria tailored for each site investigated (Gucunski and Woods, 1991; Stokoe et al., 1994). Optimizing these criteria is challenging because of the degree of changes possible in near-surface materials. Besides the uniqueness of each site, inherent difficulties exist when evaluating and distinguishing signal from noise with only a pair of receivers. The necessity of recording repeated shots into multiple field deployments for a given site increases the time and labor requirements over a multichannel procedure. Multichannel analysis of surface waves (MASW) tries to overcome the few weaknesses of the SASW method.

The entire process classically used to produce a v_s profile through spectral analysis of surface waves involves three steps: acquisition of ground roll, construction of dispersion curve (a plot of phase velocity versus f), and backcalculation (inversion) of the v_s profile from the calculated dispersion curve. Broadband ground roll must be produced and recorded with minimal noise to accurately determine the v_s profile. A variety of techniques have been used to calculate dispersion curves (McMechan and Yedlin, 1981; Stokoe et al., 1994), each having its own unique advantages and disadvantages. Backcalculation of the v_s profile (inversion of the dispersion curve) is accomplished iteratively, using the measured dispersion curve as a reference for either forward modeling (Stokoe et al., 1994) or a least-squares approach (Nazarian, 1984). Values for Poisson's ratio and density are necessary to obtain a v_s profile from a dispersion curve and are usually estimated from local measurements or material types.

A variety of wave types are produced during the generation of planar, fundamental-mode Rayleigh waves. Among these are body waves, nonplanar surface waves, backscattered waves, and ambient noise. Body waves can manifest themselves on a shot record in a variety of ways. Refracted and reflected body waves result from interactions between body waves and acoustic impedance or velocity contrasts in the subsurface, while direct body waves travel, as the name implies, directly from the source to a receiver. Also of consequence are surface waves that have propagated only a short distance from the source. These waves usually behave in a complicated nonlinear pattern and cannot be treated as plane waves (Stokoe et al., 1994). Backscattered surface waves can be prevalent on the shot gather if horizontal discontinuities such as building foundations, earth berms, or retaining walls exist nearby (Sheu et al., 1988). Relative amplitudes of each noise type generally change with frequency and distance from the source (source offset). Each noise type normally has distinct velocity and attenuation properties that can be identified on multichannel records by the coherency pattern, arrival time, and amplitude of each.

Decomposition of recorded wavefields into a swept-frequency format permits identification of most noise by frequency phase and source offset. Decomposition can therefore be used in association with multichannel records to make adjustments to minimize noise during acquisition. Selection of data-processing parameters such as the optimum frequency range for the phase-velocity calculation can be made more accurately from multichannel shot records. Once shot gathers are decomposed, a simple multichannel coherency measure applied in the time (Yilmaz, 1987) or frequency domain (Park et al., 1998b) can be used to calculate phase velocity with a frequency. Phase velocity with frequency are the two variables (x, y) that make up the dispersion curve. It is also possible to determine the accuracy of the calculated dispersion curve by analyzing the linear slope of each frequency component of the ground roll on a single shot gather. In this way, MASW allows the optimum recording and separation of broad bandwidth and high S/N ratio Rayleigh waves from other acoustic energy. A high S/N ratio ensures accuracy in the calculated dispersion curve, while the broad bandwidth improves resolution and possible depth of investigation of the inverted v_s profile (Rix and Leipski, 1991).

GENERAL PROCEDURE

Ground roll is easily generated by either a swept source like a vibrator or an impulsive source like a sledgehammer. Raw uncorrelated data are optimum for multichannel analysis; therefore, swept sources are preferred if they can be frequency and amplitude optimized for the target. Impulsive source data, on the other hand, need to be decomposed into a swept-frequency format to expose phase velocity-frequency relationship of dispersive ground roll. The basic field configuration and acquisition routine for MASW is generally the same as that used in conventional common midpoint (CMP) body-wave reflection surveys. Some rules of thumb for MASW are inconsistent with reflection optimization. This commonality allows development of near-surface velocity field variations using MASW that can be used for accurate statics corrections on reflection profiles. MASW can be effective with as few as twelve recording channels connected to single low-frequency geophones (<10 Hz).

Near offset

Even with the dominance of ground roll on seismic data, optimal recording of ground roll requires field configurations and acquisition parameters favorable to recording planar, fundamental-mode Rayleigh waves and unfavorable to all other types of acoustic waves. Because of undesirable near-field effects, Rayleigh waves can only be treated as horizontally traveling plane waves after they have propagated a certain distance (offset x_1) from the source point (Richart et al., 1970). Plane-wave propagation of surface waves does not occur in most cases until the near-offset (x_1) is greater than half the maximum desired wavelength (λ_{max}) (Stokoe et al., 1994):

$$x_1 \geq 0.5\lambda_{max}. \quad (1)$$

On a multichannel record displayed in a swept-frequency format, near-field effects manifest themselves as a lack of linear

coherency in phase at lower frequencies. This effect manifests itself as arrivals with increased frequencies that lack coherency (Figure 1b). Different investigators have reported different optimum ratios between x_1 and λ_{max} (Gucunski and Woods, 1991; Stokoe et al., 1994). The normally accepted axiom is that the penetration depth (z_λ) of ground roll is approximately equal to its wavelength (λ) (Richart et al., 1970), while the maximum depth (z_{max}) for which v_s can be reasonably calculated is about half the longest wavelength (λ_{max}) measured (Rix and Leipski, 1991). Rewriting equation (1) to represent maximum depth,

$$x_1 \geq z_{max} \tag{2}$$

provides a good rule of thumb for selecting near-offset distances.

Far offset

As with all acoustic energy traveling in the earth, high-frequency (short-wavelength) components of surface waves attenuate quite rapidly with distance away from the source (Bullen, 1963). If the maximum receiver offset is too large, the high-frequency components of surface-wave energy will not dominate higher-frequency components of the spectrum—specifically, body waves. Contamination by body waves because of attenuation of high-frequency ground roll at longer offsets is referred to here as the far-offset effect. Far-offset effects manifest themselves as a decrease in ground roll slope (increased apparent phase velocity) or reduction in the linear coherency of a band of arrivals because of interference between low-velocity ground roll and high-velocity body waves (Figure 1c). Far-offset effects initially are evident at far-offset traces, spreading inward with increasing frequency to near-offset traces. This effect limits the highest frequency (f_{max}) at which phase velocity can be measured. When the initial layer model is created according to the half-wavelength criterion, f_{max} usually designates the uppermost thickness (H_1) imaged for a particular measured phase velocity (Stokoe et al., 1994):

$$H_1 \geq 0.5\lambda_{min} = 0.5C_{min}/f_{max}, \tag{3}$$

where C_{min} and λ_{min} are phase velocity and wavelength, respectively, corresponding to a particular f_{max}. Although the final inverted v_s profile may possess shallow layers thinner than H_1, calculated v_s values for these layers should be considered unreliable (Rix and Leipski, 1991). Equation (3) can be used as a rough estimation of the minimum definable thickness of the shallowest layer. If a smaller H_1 is sought, the receiver spread and/or offset from the source needs to be reduced (decrease x_1 and/or decrease receiver spacing dx). To avoid spatial aliasing, dx cannot be smaller than half the shortest wavelength measured.

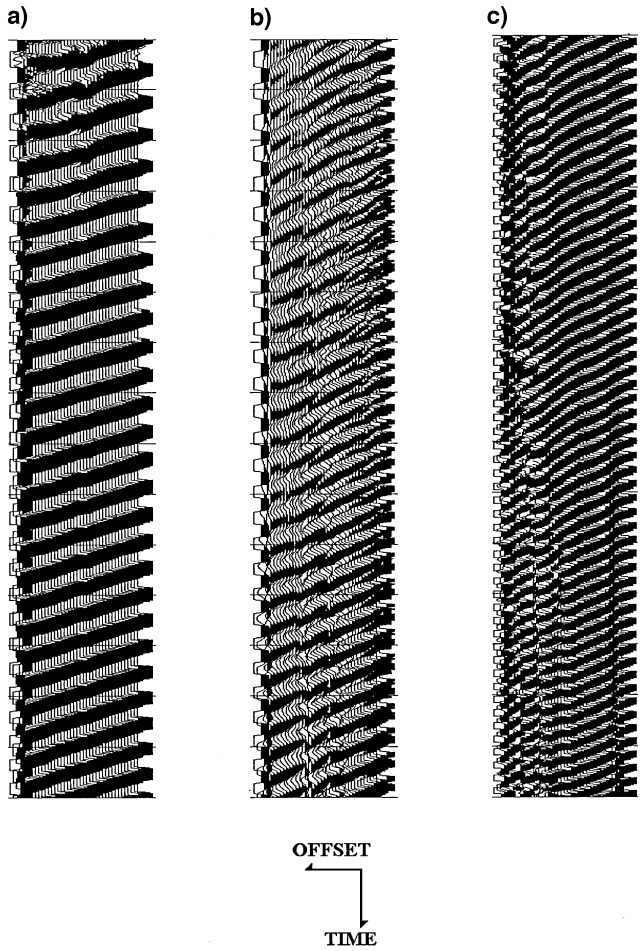

FIG. 1. Field data examples of different quality in recorded ground roll obtained using Vibroseis. [The first trace represents the sweep used.] Ground roll is shown with distinctive coherency over most traces in (a), indicating a good quality, whereas it suffers from (b) near-field effect that is identified by either weak energy or reduced coherency with fragmented energy packets and (c) far-offset effect that is identified by decreased slopes in comparison to earlier lower-frequency components or reduced coherency. The distance (x_1) of the nearest receiver from the source is (a) 27 m, (b) 1.8 m, and (c) 89 m.

Swept-frequency record

A swept-frequency record can be obtained either directly (an uncorrelated Vibroseis field record) or indirectly (an impulsive record passed through a stretch function). Three parameters need to be considered when preparing a swept-frequency record: the lowest frequency recorded (f_1), the highest frequency recorded (f_2), and length (T) of frequency-time plot or stretch function. Optimum selection of these parameters should be based on a series of rules of thumb.

It has been suggested that the lowest frequency (f_1) analyzed determines the maximum depth of investigation z_{max} such that

$$z_{max} = C_1/(2f_1), \tag{4}$$

where C_1 is phase velocity for frequency f_1 (Rix and Leipski, 1991). The lowest frequency recorded is usually limited by the natural frequency of the geophone and source type/configuration. If z_{max} is not sufficient to meet the depth requirement, a different type of source should be tested that has the potential to generate more low-frequency energy and/or lower-frequency geophones should be used.

The highest frequency to be analyzed (f_2) should initially be chosen higher than likely necessary (several times higher than the apparent frequency of ground roll) and lowered to the optimal value after noise analysis.

Length (T) of the swept-frequency record should be as long as feasible or possible, allowing detailed examination of changes in ground roll frequency. A longer T is necessary when near-surface properties change rapidly with depth. When f_1

and f_2 are properly selected, a T of no more than 10 s is sufficient.

Stretch function

An impulsive record $r(t)$ obtained by using a source such as a sledgehammer or weight drop can be transformed into the swept-frequency record $r_s(t)$ by convolution of $r(t)$ with a stretch function $s(t)$ (Coruh, 1985):

$$r_s(t) = r(t)^* s(t), \tag{5}$$

where * denotes the convolution operation. The stretch function $s(t)$ is a sinusoidal function with changing frequency as a function of time. A linear sweep similar to those commonly used in Vibroseis surveys (Waters, 1978) is a good choice for $s(t)$:

$$s(t) = \sin\left(2\pi f_1 t + \frac{\pi(f_2 - f_1)}{T} t^2\right), \tag{6}$$

where f_1, f_2, and T are lowest, highest, and length of $s(t)$. These parameters can be optimized using the previously outlined procedure.

Dispersion curve

Generation of a dispersion curve is one of the most critical steps for eventually generating an accurate shear-wave velocity profile. Dispersion curves are generally displayed as phase velocity versus frequency. This relationship can be established by calculating the phase velocity from the linear slope of each component of the swept-frequency record. The accuracy of a dispersion curve can be enhanced by the analysis and removal of noise on ground roll data. With the excellent isolation potential of each frequency component, a multichannel coherency measure (Yilmaz, 1987) can be applied to a ground roll seismogram. A frequency-domain approach (Park et al., 1998b) to calculating the dispersion curve can also be used on impulsive data.

Inversion

The v_s profiles are calculated using an iterative inversion process that requires the dispersion data and estimations of Poisson's ratio and density. A least-squares approach allows automation of the process (Xia et al., 1999). For the method used here, only v_s is updated after each iteration, with Poisson's ratio, density, and model thickness remaining unchanged throughout the inversion.

An initial earth model needs to be specified as a starting point for the iterative inversion process. The earth model consists of velocity (P-wave and S-wave velocity), density, and thickness parameters. Among these four parameters, v_s has the most significant effect on the reliable convergence of the algorithm. Several methods are reported to ensure the reliable and accurate convergence after calculating the initial v_s profile (Heukelom and Foster, 1960; Vardoulakis and Vrettos, 1988). An initial v_s profile should be defined such that v_s at a depth z_f is 1.09 times (Stokoe et al., 1994) the measured phase velocity C_f at the frequency where wavelength λ_f satisfies the relationship

$$z_f = a\lambda_f, \tag{7}$$

where a is a coefficient that only slightly changes with frequency and is based on extensive modeling (Figure 5c). One inversion method (Xia et al., 1999) guarantees the process procedure converges to a reliable result for a wide range of initial models.

FIELD TEST WITH SWEPT SOURCE

An IVI Minivib was used to generate swept surface-wave (ground roll) data at a test site near the Kansas Geological Survey in Lawrence, Kansas. The main purpose of this field test was to produce a v_s profile using the MASW procedure. The site consists of a thick (>50 m) layered shale sequence overlying a repetitive section of Kansas cyclothems (Moore, 1964). The surface topography was relatively flat with only subtle relief, <1 m across the 100-m-long site. The weathered-zone thickness was known to be about 3 m.

Forty-one of the 48 channels available on a Geometrics Strataview seismograph were connected to a group of three 10-Hz Geospace geophones with each group separated by 1 m. During the survey design, the thickness of the uppermost layer to be resolved was chosen to be about the same as the thickness (3 m) of the weathered zone. The minimum offset (x_1) was chosen to be 1.8 m to allow observation of the near-field effect. A 10-s linear upsweep from 10 to 50 Hz was recorded with a 1-ms sampling interval. A maximum depth of investigation was chosen not in advance but after noise analysis was assigned, so as to be consistent with the lowest measured frequency (10 Hz).

Shot gathers from our test site suffer from severe near-field effects at low frequencies (<about 25 Hz), as indicated by the lack of ground roll coherency (Figure 2). The slightly curved nature of the coherent ground roll events is believed to be from a slight topographic high (<1 m) near the center of the line or a laterally variable velocity structure. Far-offset effects are noticeable at higher frequencies (>about 40 Hz) and longer offsets. Subsequent processing suggests these effects do not adversely affect the accuracy of calculated phase velocities at the higher frequencies. The lowest observed phase velocity was about 200 m/s at 50 Hz, equating to a minimum wavelength of 4 m. Half this minimum wavelength is comparable to the expected thickness of the uppermost layer, or the shallowest depth of investigation for this data.

Subsequent noise analysis attempts were designed to estimate the highest recorded phase velocity without near-field effect. A minimum offset x_1 was chosen large (89 m) to enhance these effects. Good coherency is observed (Figure 3) for frequencies from about 20 Hz down to near the natural frequency of the geophones (10 Hz). The reduced coherency evident near 10 Hz (near 500 ms recording time) is not because of the near-field effect but is rather from the purposely tapered drive force of the vibrator at the start of the sweep (necessary because of physical limitations of the vibrator) and ambient noise. The highest phase velocity was about 800 m/s for frequencies very near 10 Hz. At later times, traces at this site suffer from high-amplitude body waves, backscatter from nearby buildings, and surface waves from vehicle traffic. Based on the previous two noise analyses, the approximate range of phase velocities measurable at this site is estimated to be 200–800 m/s,

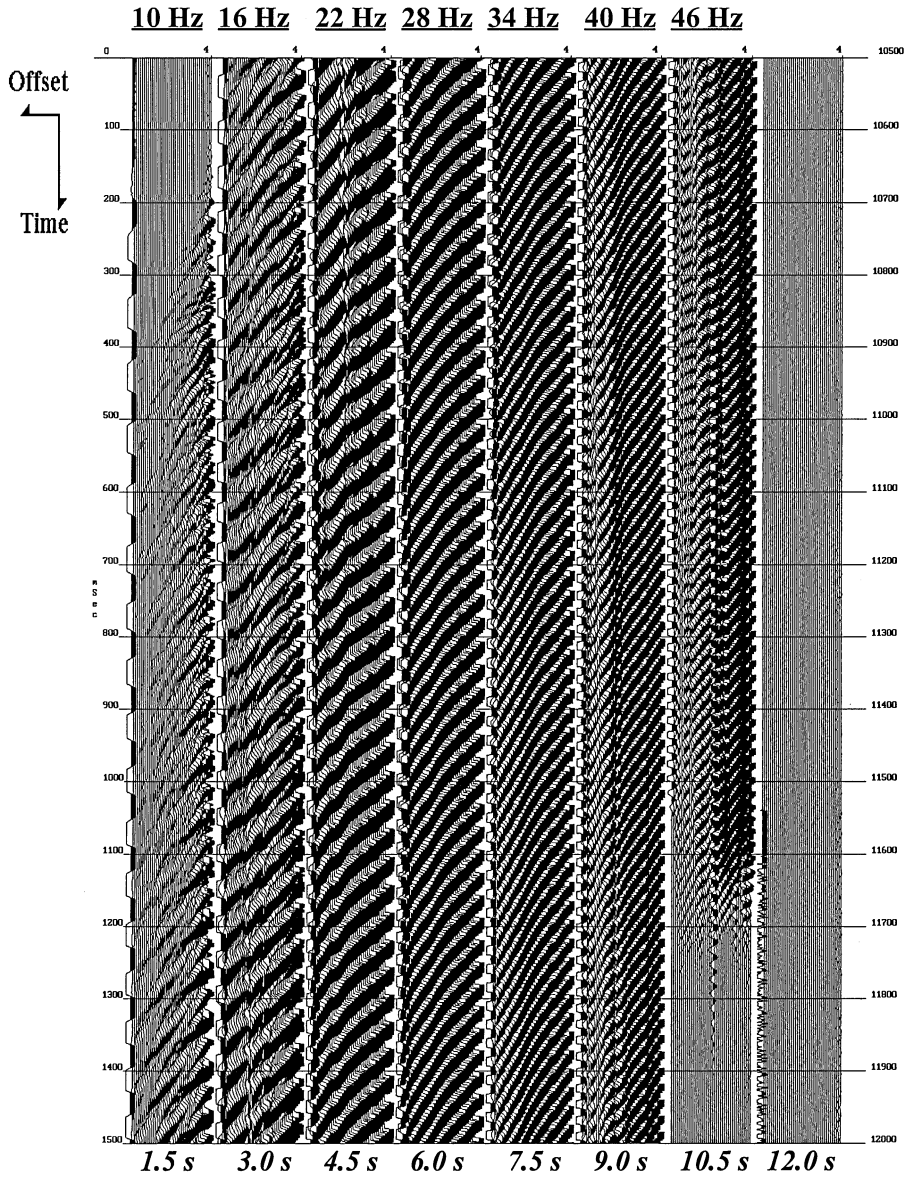

FIG. 2. Uncorrelated field record obtained using a source offset (x_1) of 1.8 m. A sweep of 10–50 Hz with 10-s sweep length was used and represented in the first trace. The record is displayed in 1.5-s segments because of the long record length. On the top and bottom of each segment are shown the sweep frequency and the time at the corresponding part of the record.

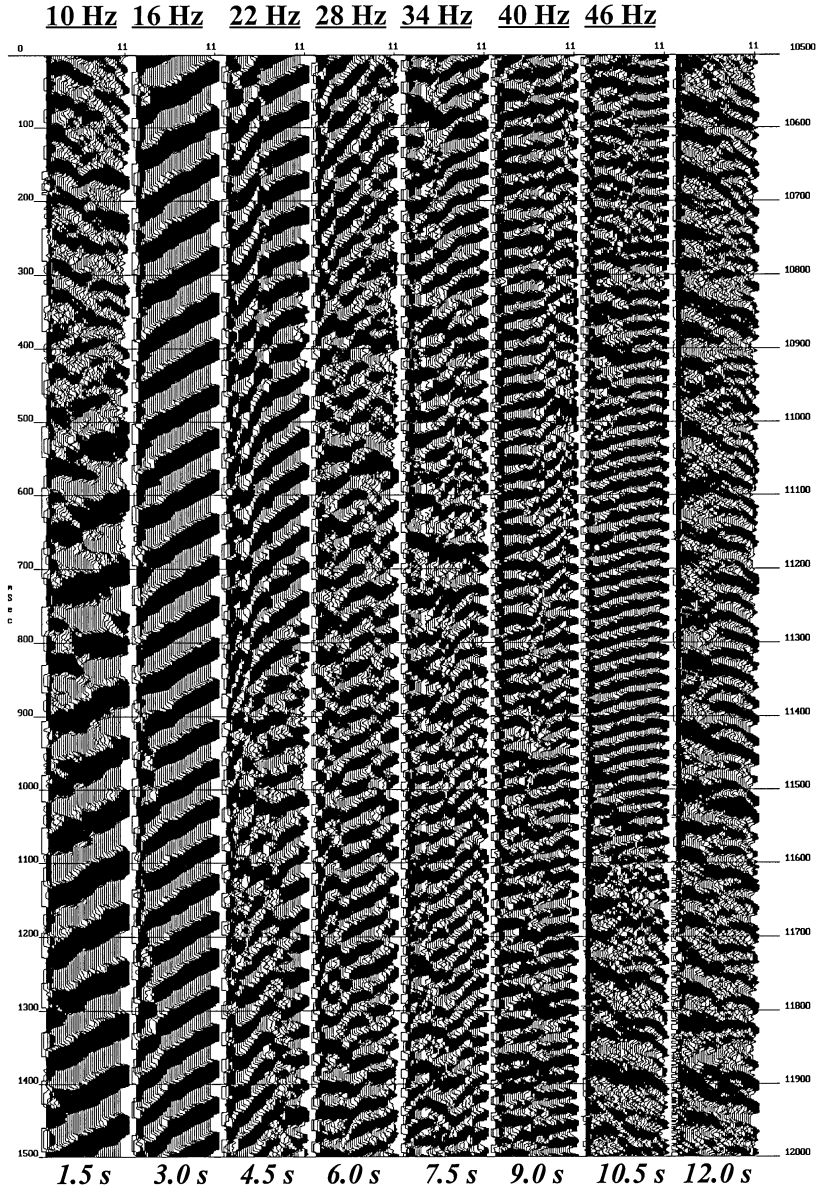

FIG. 3. Uncorrelated field record obtained by using a source offset (x_1) of 89 m.

corresponding to a wavelength range of 4–80 m and resulting in a 40-m maximum depth (z_{max}) of investigation.

A third record (Figure 4) was acquired with an x_1 (27 m) smaller than suggested by equation (2). This was done for two reasons. First, from the two previous noise analyses the optimum ratio between x_1 and λ_{max} (avoiding near-field effects [equation (1)]) turned out to be about 0.3 (instead of the predicted 0.5). Second, the dominance of far-offset effects increased rapidly with offset, indicating the farthest offset needs to be closer to the source. This third record possesses a broadband ground roll spectra and suffers the least from near-field and far-offset effects of the three records from this site (Figures 2–4). Far-offset effects at frequencies higher than about 35 Hz did not affect the calculated phase velocities, indicative of a minimal noise environment (Park et al., 1998b).

The inverted v_s profile compares quite well with a nearby downhole-measured v_s profile (Figure 5a). A test well located near the end of the geophone spread was used to produce the measured downhole v_s profile using a three-component downhole receiver and a sledgehammer source. The downhole profile was calculated to be consistent with the thickness model used in the inversion process. Less than a 7% overall deviation can be observed between the inverted v_s profile and the downhole v_s profile. The close match between the inverted earth model and the measured data in terms of dispersion property is quite encouraging and provides a reasonable measure of ground truth (Figure 5b).

FIELD TEST WITH IMPULSIVE SOURCE

The flexibility of this technique is demonstrated by impulsive data acquired at Geometrics' San Jose, California, test site (Figure 6a). Data from this site were recorded using a sledgehammer source and 4.5-Hz geophones. A swept-frequency record can be transformed from the impulsive record (Figure 6b). The first trace in this record represents the stretch function used

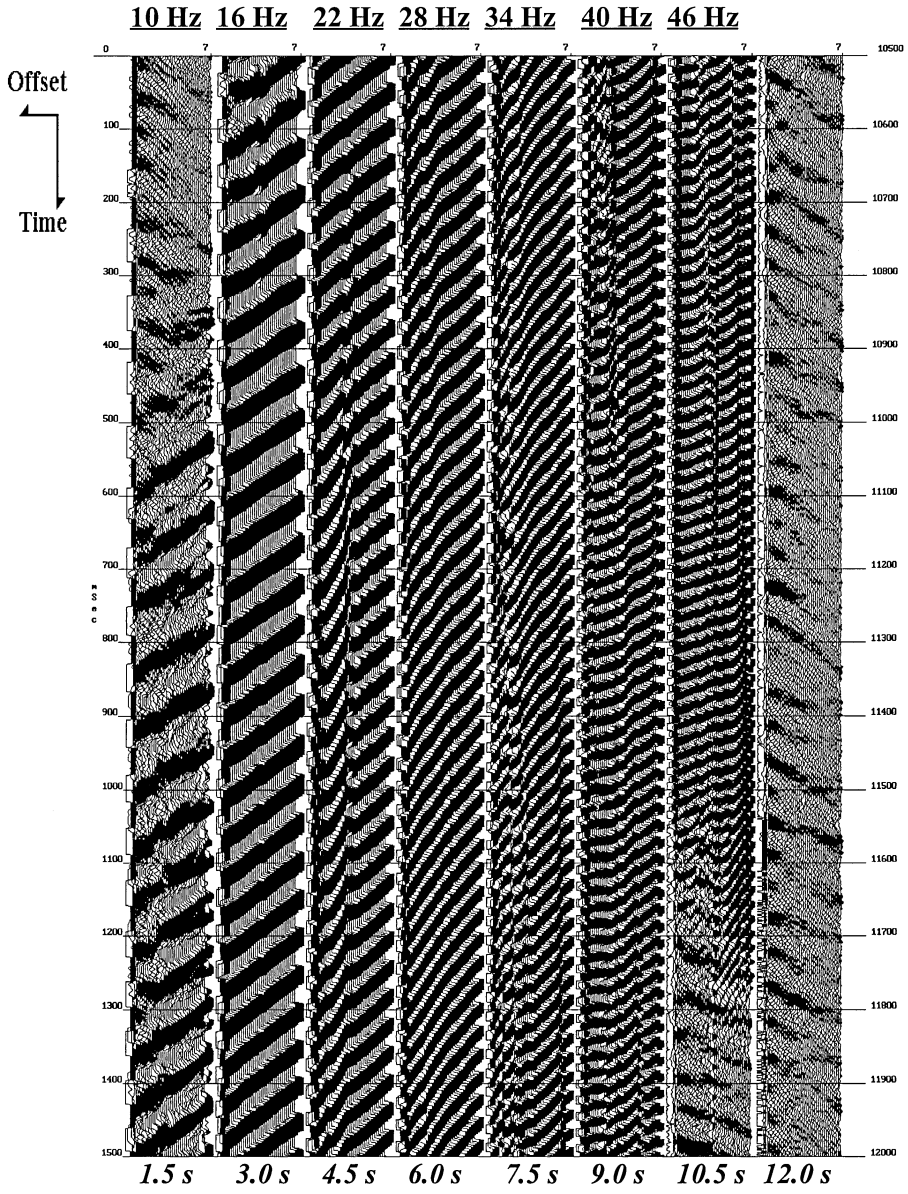

FIG. 4. Uncorrelated field record obtained by using a source offset (x_1) of 27 m.

to linearly separate frequencies from 5 to 55 Hz across the 2.5-s record. Near-field effects are obvious at low frequencies (<10 Hz) on these data. Little energy appears to have propagated to far-offset (>50 m) traces. Far-offset effects are obvious at high frequencies (>25 Hz) as well on these data. Far-offset effects manifest themselves on these data as severe attenuation (25–45 Hz) and body-wave contamination (>45 Hz) on longer-offset (>30 m) traces. For these reasons, near-offset (4–30 m) and far-offset (30–60 m) traces were digitally separated for phase-velocity calculations. This would be equivalent to acquiring and processing two shot gathers with fewer traces and into different spreads. The calculated dispersion curve (Figure 7a) obtained by analyzing only the far-offset traces shows a reasonable trend at the lower frequencies (<15 Hz), but body-wave contamination corrupts the trend at higher frequencies. The lowest analyzable frequency in this dispersion curve is around 3 Hz. The dispersion curve (Figure 7a) obtained by analyzing only near-offset traces provides a realistic trend for most frequencies above 6 Hz.

The two dispersion curves (Figure 7a) were combined to form a composite dispersion curve (Figure 7c), which was used to generate the v_s profile (Figure 7b).

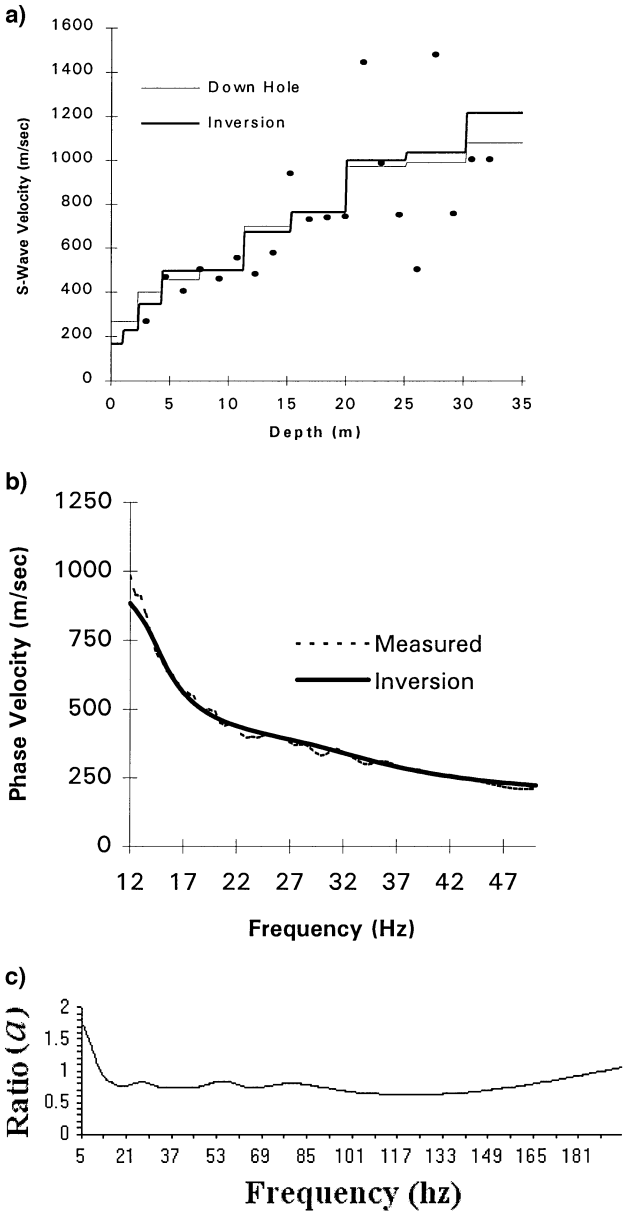

FIG. 5. Inversion results from a field test of (a) a v_s profile and (b) the corresponding dispersion curve in comparison with a downhole v_s profile and measured dispersion curve. Dots in the displayed v_s profile in (a) represent the data points actually measured during the downhole survey. The downhole profile was recalculated from these data according to the thickness model used in the inversion process. (c) The ratio a in equation (7) that was used during construction of the initial v_s profile.

DISCUSSIONS

The MASW method emphasized the minimization of near-field and far-offset effects, acquisition speed, sampling redundancy, and overall data accuracy. Minimization of near-field and far-field effects is achieved through optimum field configuration and/or a selective offset and frequency processing.

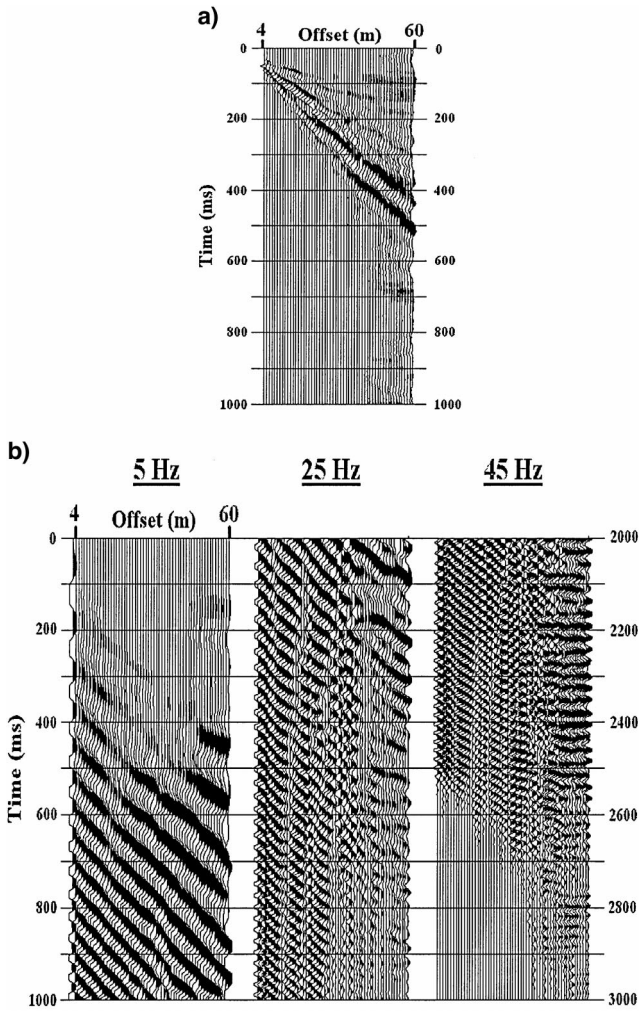

FIG. 6. (a) A shot gather obtained using a 12-lb sledgehammer as the source at a soil site in San Jose, California, and (b) its 3-s-long swept-frequency display after transformation using a stretch function (first trace). The swept-frequency record is displayed in 1-s segments. On top of each segment are shown the frequencies of the stretch function at the corresponding parts of the record.

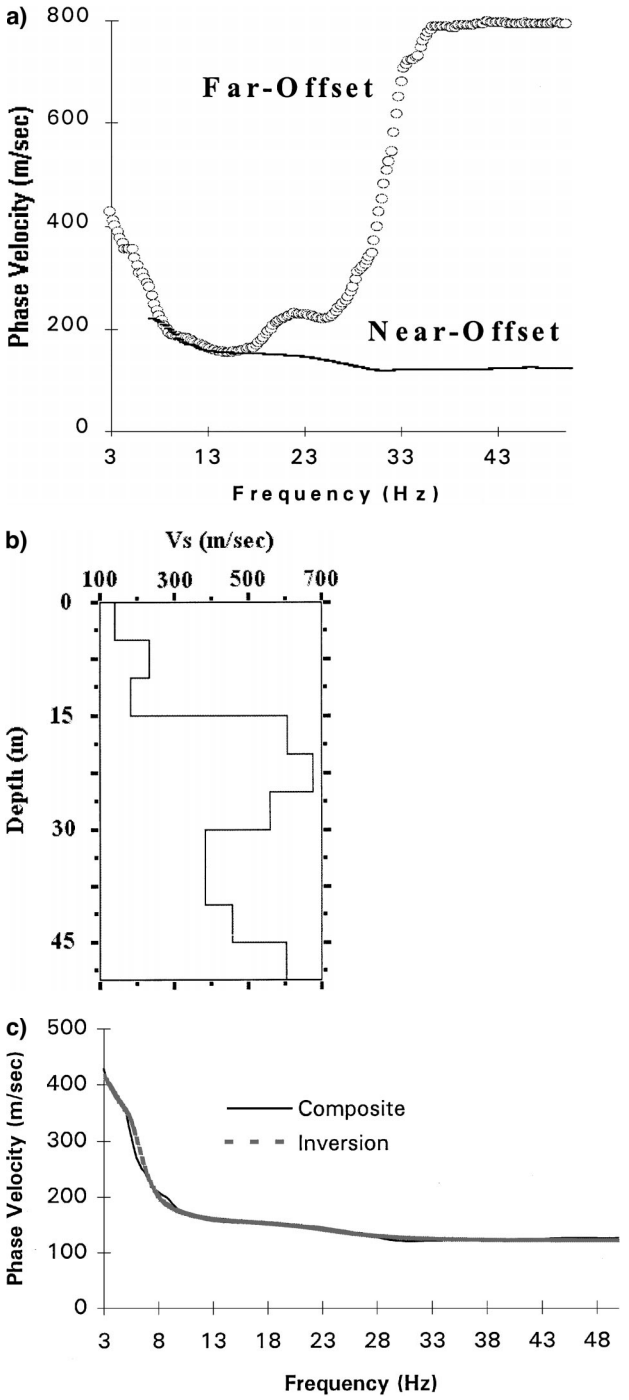

FIG. 7. (a) Dispersion curves obtained by processing near-offset (4–30 m) traces and far-offset (30–60 m) traces of the record in Figure 6a separately. (b) A v_s profile obtained from the inversion of a composite dispersion curve created by integrating the two curves. (c) The composite dispersion curve in comparison with the dispersion curve corresponding to the inverted v_s profile in (b).

Sampling redundancy is obtained by the relatively large number and tight spacing of all receivers. Accuracy of the MASW method was tested through ground truth comparisons with borehole measurements.

MASW assumes that the nature of near-surface materials can be treated implicitly as a layered earth model with no lateral variation in elastic properties. It is therefore important to keep the entire spread as short as possible to maximize the validity of this assumption if lateral variations are suspected. From an empirical perspective, this assumption is valid as long as good linear coherency is observed on decomposed or swept shot records.

We do not see any appreciable difference in the overall effectiveness, whether using a swept source or an impulsive source. Considering the relative importance of lower frequencies for deeper penetration, a heavy impulsive source seems to be an effective and economic choice. Because of this dependence on depth of penetration in the lower frequencies, we recommend always using high-output, low-frequency geophones with no recording filters. As far as the stretch function or Vibroseis sweep is concerned, we see no difference in the resulting v_s profile between up or down sweeps.

A frequency-continuous approach makes the swept-frequency display more useful when analyzing the interaction between several different types of seismic events, as compared with conventional filter panels. The optimum offset and lowest usable frequency outside the ground roll can be established more effectively using a swept-frequency display than from the impulsive record alone. This makes decomposition of frequencies a potentially useful tool for compressional surveys as well.

An indication of the overall speed of the MASW process is revealed by the production of a ten-layer v_s profile in less than 5 minutes on a 100-MHz Pentium-based PC from a 48-channel, 12-s-long swept-frequency record.

CONCLUSIONS

When ground roll is acquired using a multichannel recording method and displayed in a swept-frequency format, different frequency components of Rayleigh waves can be identified by distinctive and simple coherency. This leads to a seismic surface-wave method that provides a useful noninvasive tool, where information about elastic properties of near-surface materials can be effectively obtained for two reasons:

1) The integrity of each single Rayleigh wave frequency can be readily examined for contamination by coherent noise, making adjustments possible to improve S/N ratio during data acquisition and processing steps, and
2) A highly accurate dispersion curve can be obtained and inverted to produce a v_s profile with high confidence and consistency using ground roll recorded on a single shot gather.

ACKNOWLEDGMENTS

We thank Joe Anderson, David Laflen, and Brett Bennett for their commitment during the field tests. A special thanks to Lee Gerhard, director of the Kansas Geological Survey (KGS), and Kathy Sheldon, chief of operations at KGS, for giving permission to acquire vibroseis data at the KGS test site. Finally, we thank Mary Brohammer for her help in the preparation of this manuscript.

REFERENCES

Bullen, K. E., 1963, An introduction to the theory of seismology: Cambridge Univ. Press.
Coruh, C., 1985, Stretched automatic amplitude adjustment of seismic data: Geophysics, **50**, 252–256.

Gucunski, N., and Woods, R. D., 1991, Instrumentation for SASW testing, *in* Bhatia, S. K., and Blaney, G. W., Eds., Recent advances in instrumentation, data acquisition and testing in soil dynamics: Am. Soc. Civil Eng., 1–16.

Heukelom, W., and Foster, C. R., 1960, Dynamic testing of pavements: J. Soil Mechanics and Foundations Div., **86**, no. SM1, 1–28.

Mari, J. L., 1984, Estimation of static corrections for shear-wave profiling using the dispersion properties of Love waves: Geophysics, **49**, 1169–1179.

McMechan, G. A., and Yedlin, M. J., 1981, Analysis of dispersive waves by wave field transformation: Geophysics, **46**, 869–874.

Moore, R. C., 1964, Paleoecological aspects of Kansas Pennsylvanian and Permian Cyclothems: Kansas Geol. Bull., **169**, no. 1, 287–380.

Nazarian, S., 1984, In situ determination of elastic moduli of soil deposits and pavement systems by spectral-analysis-of-surface-waves method: Ph.D. dissertation, Univ. of Texas, Austin.

Nazarian, S., Stokoe, K. H., II, and Hudson, W. R., 1983, Use of spectral analysis of surface waves method for determination of moduli and thicknesses of pavement systems: Transport. Res. Record, **930**, 38–45.

Park, C. B., Xia, J., and Miller, R. D., 1998a, Ground roll as a tool to image near-surface anomaly: 68th Ann. Internat. Mtg., Soc. Expl. Geophys., Expanded Abstracts, 874–877.

———1998b, Imaging dispersion curves of surface waves on multichannel record: 68th Ann. Internat. Mtg., Soc. Expl. Geophys., Expanded Abstracts, 1377–1380.

Richart, F. E., Hall, J. R., and Woods, R. D., 1970, Vibrations of soils and foundations: Prentice-Hall, Inc.

Rix, G. J., and Leipski, E. A., 1991, Accuracy and resolution of surface wave inversion, *in* Bhatia, S. K., and Blaney, G. W., Eds., Recent advances in instrumentation, data acquisition and testing in soil dynamics: Am. Soc. Civil Eng., 17–32.

Sheu, J. C., Stokoe, K. H., II, and Roesset, J. M., 1988, Effect of reflected waves in SASW testing of pavements: Transportation Res. Record, **1196**, 51–61.

Stokoe, K. H., II, Wright, G. W., James, A. B., and Jose, M. R., 1994, Characterization of geotechnical sites by SASW method, *in* Woods, R. D., Ed., Geophysical characterization of sites: Oxford Publ.

Vardoulakis, I., and Vrettos, C., 1988, dispersion law of Rayleigh-type waves in a compressible Gibson half space: Internat. J. Numerical and Analytical Methods in Geomechanics, **12**, 639–655.

Waters, K. H., 1978, Reflection seismology: John Wiley & Sons, Inc.

Xia, J., Miller, R. D., and Park, C. B., 1999, Estimation of near-surface shear-wave velocity by inversion of Rayleigh wave: Geophysics, **64**, 691–700, this issue.

Yilmaz, O., 1987, Seismic data processing: Soc. of Expl. Geophys.